Published in final edited form as:
Electrophoresis. 2012 December ; 33(24): 3728–3737. doi:10.1002/elps.201200251.

SILAC-based proteomic analysis to investigate the impact of amyloid precursor protein expression in neuronal-like B103 cells

Dale Chaput[1], **Lisa Hornbeck Kirouac**[2], **Harris Bell-Temin**[1], **Stanley M. Stevens Jr**[1,*], and **Jaya Padmanabhan**[2,*]

[1]Department of Cell Biology, Microbiology, and Molecular Biology, University of South Florida, Tampa, Florida, USA

[2]Department of Molecular Medicine, USF Health Alzheimer's Institute, University of South Florida, Tampa, Florida, USA

Abstract

Alzheimer's disease (AD) is the most prevalent form of dementia in the elderly. Amyloid plaque formation through aggregation of the amyloid beta peptide derived from amyloid precursor protein (APP) is considered one of the hallmark processes leading to AD pathology; however, the precise role of APP in plaque formation and AD pathogenesis is yet to be determined. Using stable isotope labeling by amino acids in cell culture (SILAC) and mass spectrometry, protein expression profiles of APP null, rat neuronal-like B103 cells were compared to B103-695 cells which express the APP isoform, APP-695. A total of 2,979 unique protein groups were identified among 3 biological replicates and significant protein expression changes were identified in a total of 100 non-redundant proteins. Some of the top biological functions associated with the differentially expressed proteins identified include cellular assembly, organization and morphology, cell cycle, lipid metabolism, protein folding, and posttranslational modifications. We report several novel biological pathways influenced by APP-695 expression in neuronal-like cells and provide additional framework for investigating altered molecular mechanisms associated with APP expression and processing and contribution to AD pathology.

Keywords

Alzheimer's Disease; amyloid beta; amyloid precursor protein; proteomics; SILAC

1. Introduction

Alzheimer's disease is the most common form of dementia that affects elderly and is associated with cognitive decline and loss of executive function. The two major pathological characteristics of the disease are the presence of neuritic plaques and neurofibrillary tangles (NFT) in the areas of the brain associated with learning and memory [1–3]. Neuritic plaques are formed by extracellular accumulation of amyloid beta, a peptide derived from amyloid precursor protein (APP). APP is a single transmembrane domain protein that is expressed at high levels in brain. Studies in Alzheimer's disease brains have shown that APP is cleaved

Corresponding Authors: Dr. Jaya Padmanabhan, University of South Florida, Department of Molecular Medicine, USF Health Byrd Alzheimer's Institute, 4001 E. Fletcher Ave., Tampa, FL 33613, jpadmana@health.usf.edu, Dr. Stanley M. Stevens Jr., University of South Florida, Department of Cell Biology, Microbiology, and Molecular Biology, 4202 E Fowler Ave, Tampa, FL 33620, smstevens@usf.edu.
*Dr. Stanley M. Stevens Jr. and Dr. Jaya Pabmanabhan are equal last authors

The authors have declared no conflict of interest.

by beta (BACE) and gamma secretases to generate amyloid beta (Aβ), a peptide fragment that is 40–42 amino acids long (Aβ40 and Aβ42) [4–8]. In addition to beta and gamma secretases, APP is also cleaved by alpha secretase; this secretase cleaves APP within the Aβ domain and thus excludes the formation of Aβ from APP. The secretase-cleavages of APP generate ectodomains and intracellular domains of APP in addition to Aβ (Fig. 1a). APP has been reported to enhance neurite outgrowth, inhibit neurodegeneration and exert anti-apoptotic activity. Of the different APP fragments, Aβ and AICD (APP intra cellular domain) have been shown to enhance neurodegeneration while the secreted alpha-cleaved ectodomain of APP (sAPPα) has been shown to have growth promoting activity.

A number of factors such as age, environment, and inflammatory proteins appear to affect the onset of Alzheimer's disease (AD). Several independent studies have shown that cell cycle deregulation correlates with pathology development in AD. Analysis of brains from AD patients and mice expressing AD transgenes have shown increased expression of cell cycle regulatory proteins in neurons, which correlated with APP and tau phosphorylation and pathology development [9–21]. We recently showed that phosphorylation and cellular distribution of APP are affected in a cell cycle-dependent manner and this is associated with altered processing of APP [10]. The discoveries demonstrating that cells expressing APP show enhanced growth rate and the observation that APP localizes to centrosomes under mitotic conditions led to the hypothesis that it may play a role in cell cycle progression. The exact role of APP in cell cycle activation and cell proliferation is not yet identified. Here we sought to determine the mechanism(s) by which APP affects cellular functions using APP null B103 nerve cells.

Elegant studies by Schubert and colleagues have shown that B103 nerve cells do not express either APP or the APP like proteins APLP1 or APLP2 [22]. Therefore, these cells are appropriate for studying the cellular functions of APP. These investigators showed that expression of APP in B103 cells enhances cell adhesion, neurite outgrowth, and cell proliferation but the molecular mechanisms by which APP induces these cellular functions are not quite clear. It is possible that APP or a metabolite of APP can induce these either by itself or by affecting expression of genes associated with these functions. In order to determine whether APP affects expression of proteins associated with cell adhesion or cell cycle progression or cell signaling processes in general, we performed an unbiased, global-scale analysis to assess APP-mediated protein expression changes in B103 cells. We used the stable isotope labeling by amino acids in cell culture (SILAC) approach for comparing the protein complement of B103 cells expressing the 695 isoform of APP (referred to as B103-695) to B103 APP null cells (referred to as B103) as shown in Fig. 1b. The advantage of this approach is that B103 cells can be grown in media containing normal or "light" versions of amino acids and B103-APP in media with "heavy" amino acids. The labeled (heavy) amino acids are added to media that are deficient in specific amino acids (in this case L-arginine and L-lysine) and the cells metabolically incorporate these amino acids during protein synthesis. This technique allows one to differentiate proteins from one cell system to the other and analyze both simultaneously using tandem mass spectrometry. This approach decreases experimental variability that occurs during sample processing and provides more consistent and reliable data for relative protein quantitation. Here we provide evidence for protein expression changes in B103 cells expressing APP-695 versus APP null cells and validate changes in selected proteins involved in cell signaling as well as cell morphology, assembly and organization.

2. Materials and Methods

2.1 Cell Culture and SILAC Labeling

B103 and B103-695 rat neuroblastoma cells were initially cultured in DMEM/F12 (1:1) media supplemented with 10% FBS, 50U/ml penicillin and 50μg/ml streptomycin, at 37°C and 5% CO_2 [23]. Cells were grown in T75 cm^2 flasks to near confluence, and then split into 3 × T75 cm^2 flasks for stable isotope labeling with heavy or light amino acids in cell culture (SILAC).

B103 and B103-695 cells were labeled for quantitation using SILAC media supplemented with 10% dialyzed FBS, pen/strep, and either L-lysine and L-arginine for B103 or $^{13}C_6$-L-Lysine 2HCl and $^{13}C_6$-$^{15}N_4$-Arginine HCl for B103-695 cells (Thermo Scientific). Cells were grown in SILAC media for 7 days, during which they were passaged once and media was changed every 48 hours, for a minimum of 5 doublings, corresponding to > 98% labeling efficiency.

Cells were collected using Trypsin-EDTA and washed 3 times with PBS to remove serum proteins. Cells were lysed in 250μl of 100mM Tris-HCl (pH 7.6) containing 4% SDS, 100 mM dithiothreitol (DTT), and Halt protease inhibitor cocktail (Pierce) at 95°C for 5 minutes. Lysed samples were briefly sonicated. Protein concentrations were determined using the Pierce 660nm protein assay with the ionic detergent compatibility reagent (Pierce). These experiments were done in triplicate.

2.2 Sample Preparation

Whole cell lysates were digested using the filter-aided sample preparation (FASP) kit (Protein Discovery), as developed by Wisniewski and Mann [24]. Four digestions of approximately 100μg of protein were performed for each biological replicate, which were then pooled for a total of 400μg per biological replicate. Thirty microliters of protein sample and 8 M urea were mixed and added to the 30kDa FASP spin filter for buffer exchange. Samples were alkylated according to manufacturer's instructions with iodoacetamide (IAA) for 30 minutes in the dark. Following alkylation, samples underwent further buffer exchange with 3 × 100 μl additions of 50 mM ammonium bicarbonate, followed by centrifugation at 14,000 × g for 10 minutes. Samples were incubated with trypsin at 1:100 (w:w, trypsin:protein) for proteolytic digestion of proteins and incubated overnight at 37°C. Peptides were collected by centrifugation with the addition of 2 × 40 μl 50 mM ammonium bicarbonate and 40 μl NaCl. Peptides were desalted using Supelco Discovery DSC-18 solid-phase extraction columns in combination with a Supelco vacuum manifold. Samples were dried using a vacuum concentrator (Thermo) and resuspended in 20 μl of 0.1% formic acid in H_2O.

Peptides were fractionated on a Dionex U3000 HPLC system with a 150 cm × 1.0 mm i.d. strong cation-exchange (SCX) column (PolyLC Inc.) packed with 5 μm 300 Å polySULFOETHYL A-SCX material. Two minute fractions were collected using a 30 minute gradient, where ammonium formate increased from 15–200 mM in 25% acetonitrile (ACN) at a flow rate of 250 μl/min. Ten peptide-containing fractions were selected for LC-MS/MS analysis from each biological replicate (n=3 total). Peptides were again dried in a vacuum concentrator and resuspended in 10μl of 0.1% formic acid in H_2O.

2.3 LC-MS/MS

SCX peptide fractions were separated on a 10 cm × 75 μm i.d. reversed-phase column (New Objective) packed with 5 μm 300 Å C18 material (ProteoPep II). Tandem mass spectrometric analysis was carried out using a hybrid linear ion trap-Orbitrap instrument

(LTQ Orbitrap XL, Thermo). A 90 minute gradient was used, where 0.1% formic acid in ACN increased from 2 to 40%, increasing to 80% at 95 minutes through 100 minutes. Orbitrap full MS scans were collected at a mass resolving power of 60,000, with positive polarity in profile mode, and a scan range of m/z 350–1500. The top 5 most abundant ions were selected for further fragmentation in the ion trap. Global settings include dynamic exclusion of 90 seconds, with an exclusion list size of 500, and a repeat count of 2.

2.4 Database Searching and Pathway Analysis

Raw files were processed in MaxQuant version 1.2.0.13, a quantitative proteomics software package for the analysis of large, high resolution MS data sets [25]. The raw files were processed and searched against the current UniprotKB database containing *Rattus norvegicus* protein sequences as well as a second MaxQuant database of known contaminants. The search parameters included a constant modification of cysteine by carbamidomethylation and variable modification of methionine oxidation. Additional parameters include multiplicity set to 2, with a heavy set of lysine-6 and arginine-10. The search tolerance was set to 8 ppm and the fragment ion mass tolerance was set to 0.5 Da with a false discovery rate (FDR) of < 1%.

Statistical analysis was carried out using Perseus software, which assesses the statistical significance of protein expression based on the approach developed by Benjamini and Hochberg [26]. A threshold q-value of 0.05 for the Benjamini-Hochberg false discovery rate was used. Functional and pathway analysis of identified proteins was carried out using Ingenuity Pathway Analysis (IPA, Ingenuity Systems).

2.5 Western Blotting

Proteins were selected for Western blot validation of protein expression changes based on significance as well as function. Twenty micrograms of B103 and B103-695 cell lysate were separated on a 15% Tris/Glycine SDS-PAGE gel, run at 90V for 90 minutes. Proteins were semi-wet transferred to a nitrocellulose membrane (Whatman) at 30V for 90 minutes. The membrane was subsequently blocked in 5% non-fat milk-TBS for 1 hour at room temperature, and washed using PBS containing Tween 20 (PBST). Primary antibodies specific for Ras (Abcam, mouse monoclonal, 1:1000), P-ERK and ERK44/42 (Cell Signaling, rabbit polyclonal, 1:1000), and actin (Sigma, mouse monoclonal, 1:7000) were diluted in 3%BSA/TBS/0.02% sodium azide and incubated overnight at 4°C. Membranes were then incubated with corresponding anti-rabbit (Pierce) and anti-mouse (Pierce) secondary antibodies for 90 minutes at room temperature and washed thoroughly. The blots were developed using the Super Signal chemiluminescence reagents (Pierce).

2.6 Immunostaining analysis

B103 and B103-695 cells were plated onto poly-lysine coated 8 chamber slides and cultured overnight in DMEM/F12 (1:1) medium with serum and Pen-Strep. After 24 hrs of culturing, cells were washed with PBS and fixed with 4% para-formaldehyde for 10 minutes at room temperature. At the end of the fixation, cells were washed and incubated in 1% BSA in TBS containing 0.1 % Triton X-100 (BSA/TBST) to block any non-specific binding. After 1 hr incubation at room temperature, γ-synuclein (Millipore, rabbit monoclonal,1:500) and actin (Sigma, mouse monoclonal, 1:500) antibodies diluted in BSA/TBST was added to the cells and incubated overnight at 4°C by gentle rocking. The slides were washed with PBS thoroughly and incubated with Alexa Fluor 488 anti-mouse and Alexa Fluor 594 anti-rabbit secondary antibodies (Invitrogen/Gibco) for 1–2 hr at room temperature in the dark. At the end of the incubation cells were washed again and incubated with 1 μg/ml Hoechst 33258, diluted in PBS, for 10 minutes at room temperature protected from light. After further washes, the slides were mounted using Fluoro-gel mounting media (Electron Microscopy

Sciences) and analyzed under a Zeiss Fluorescent microscope using AxioVision Rel 4.8 software program.

3. Results and Discussion

3.1 B103 and B103-695 proteome comparison

A total of 2979 protein groups were identified among 3 biological replicates, excluding contaminants and false positive (reverse sequence) identifications (listed in Supplementary Table 1). Biological replicates A, B, and C identified 2549, 2335, and 2542 protein groups, respectively. Over 1900 protein groups were shared by all 3 biological replicates. Replicates A and B shared 2053, replicates A and C shared 2228, and replicates B and C shared 2080 protein groups. The overlap of protein identifications between biological replicates is demonstrated by the Venn diagram shown in Fig. 2.

Perseus was used to identify proteins with statistically significant changes in expression across multiple biological replicates. Two significance tests were employed, Significance A and Significance B, where the A significance gives no weight to signal intensity and B significance is weighted by signal intensity. Significance A test identified 79 significant proteins, while 83 significant proteins were identified using Significance B, for a combined total of 100 non-redundant proteins that were differentially expressed in B103-695 cells (listed in Supplementary Table 2). Of the 100 differentially expressed proteins, 8 proteins were downregulated and 92 proteins were upregulated.

3.2 Functional enrichment

Several proteins that are important in cellular and molecular functions including cellular assembly and organization, cell cycle, cell morphology, lipid metabolism, protein folding, and post translational modifications were identified as having differential expression upon proteome comparison in B103 and B103-695 cells using IPA (Fig. 3). Lipids and lipid carriers have been shown to play a role in AD pathology development. People with high cholesterol levels are at high risk of developing AD and studies in mouse models of AD have shown that drugs that lower cholesterol levels can reduce the levels of A-beta and therefore plaque pathology [27]. Studies in AD patients have shown that people carrying the apolipoproteins E4 allele (ApoE4) are more prone to get the disease than those carrying apolipoprotein E2 or E3 allele. ApoE is the major apolipoprotein in the brain and is the protein component of the lipids such as very low density lipoprotein (VLDL). Although this led to the hypothesis that ApoE4 is a genetic risk factor for AD it does not mean that all the ApoE4 carriers do get the disease. The exact mechanism by which ApoE4 affects pathology development in AD is not clear. It has been shown that ApoE4 promotes the aggregation of amyloid β and therefore accelerates plaque pathology and cognitive deficit. Lipids seem to play a role in not only the aggregation of amyloid β but also its generation. Studies have shown that APP, beta-secretase (BACE) and γ-secretase co-localize in the lipid rich raft domains leading to enhanced amyloidogenic processing of APP whereas α-secretase-mediated cleavage occurs at membrane domains outside of the lipid rafts. Regarding proteins associated with lipid metabolism, our analysis showed that the sterol O-acetyl transferase 1 (SOAT1) and Acyl CoA: cholesterol acyl transferase 2 (ACAT2) are induced by ~2.5 to 3 fold in B103-695 cells. Studies by others have shown that an increase in SOAT1 is associated with an increase in APP processing to generate amyloid β, and a downregulation of SOAT1 using siRNA descreased generation of amyloid β, suggesting a role for this enzyme in pathology development in AD. Similarly, studies have shown that ACAT2 can more efficiently esterify cholesterol than ACAT1, which is more efficient in esterification of sitosterol [28]. This again suggests that the cholesterol modifying enzymes are induced by APP expression in B103 cells implying a role for APP in altered lipid

metabolism. Many of the proteins identified are also involved in regulating physiological system development and function processes such as connective tissue, cardiovascular system, and nervous system development and function, as well as embryonic tissue development (Fig. 3).

IPA also identified significant canonical pathways associated with a number of identified proteins that were differentially expressed including CDK5 signaling, cell cycle G2/M DNA damage checkpoint regulation, actin cytoskeleton signaling, protein kinase A signaling and ERK5 signaling as shown in the selected canonical pathways in Fig. 3. CDK5 signaling is involved in cell differentiation and morphology regulation and has been implicated in neuron degeneration [29]. CDK5 signaling is important for proper brain development and dysregulation in CDK5 leads to defects in cell migration, plasticity, and other neurological defects [5][30–32]. Additionally, actin cytoskeleton and protein kinase A signaling were also over-represented from the SILAC dataset. Actin cytoskeleton signaling is associated with cell motility, axon guidance, cellular assembly, organization, function, and maintenance whereas protein kinase A is a serine/threonine kinase that functions as a second messenger regulating a variety of diverse functions including growth, development, and memory. Interestingly, the G2/M DNA damage checkpoint was identified as a potential altered pathway from the SILAC dataset as well and provides additional evidence of the involvement of cell cycle-dependent mechanisms upon APP expression in this cell model system. The G2/M DNA damage checkpoint is the second checkpoint within the cell cycle and is important for maintaining genomic stability as it prevents damaged DNA from entering M-phase.

3.3 Pathway analysis reveals APP-mediated alterations in cell morphology and Ras signaling

The top protein interaction network identified using IPA is primarily involved in cell morphology, assembly, and organization, as well as nervous system development and function which is shown in Fig. 4. Proteins of particular interest include γ-synuclein and Ras, which are both found to be upregulated in B103-695 cells. Western blots were performed to validate the increased expression of γ-synuclein and Ras in B103-695 cells. While Ras showed a significant increase by western blot analysis (Fig 5b), we were unable to detect the γ-synuclein with this technique. We believe that this is due to the limited antibody reactivity on western blots as immunostaining analysis using the anti-γ-synuclein antibody showed a significant increase in this protein in B103-695 cells compared to B103 (Fig. 5a). Co-staining of the cells with an actin antibody showed altered actin staining in B103-695, providing some additional support to the functional enrichment analysis results in which actin cytoskeleton signaling and subsequent cytoskeletal organization could potentially be altered through APP expression.

Gamma synuclein, a member of the synuclein family, was the most significantly up-regulated protein, showing a 59.6 fold increase. Increased expression of γ-synuclein mRNA has been observed in the brains of Alzheimer's disease patients, supporting its potential contribution in AD pathology [33]. γ-synuclein has also been shown to bind microtubule and promote tubulin polymerization and cell adhesion [34]. Studies in cancer cells have shown that it enhances cell migration and protects against mitotic inhibitor-mediated apoptosis. It was initially identified as a breast cancer specific gene (BCSG1) and was associated with breast tumor progression [35, 36]. γ–synuclein has been shown to interact with the checkpoint protein BubR1 to bring about the defects in mitosis [37, 38].

Ras, a small GTPase, is involved in signal transduction regulating cell growth, differentiation, and survival. Increased Ras expression has been implicated in AD brains but the functional significance of this in AD pathology development is not known [39].

Interestingly, nerve growth factor receptor (NGFR) protein in the plasma membrane, which is upregulated in our dataset as a result of APP expression in B103 cells, has been shown to increase activation of Ras protein(s) in the cytoplasm [40]. Ras activation consequently results in increased MAP-kinase activity. It is possible that a Ras-mediated cell signaling cascade may play a role in the aberrant cell cycle activation and neurodegeneration associated with pathology development in AD.

MAPK functions downstream from Ras in signal transduction pathway and responds to extracellular signals by inducing different cellular functions such as proliferation, mitosis, differentiation and apoptosis. Ras activation of the mitogen-activated protein kinase (MAPK) signaling pathway has been well established. Although the Ras – MAPK signaling pathway has a well-known role in cancer, there is increasing evidence for its involvement in neurodegenerative disease as well [41]. The Ras – MAPK signaling pathway has been found to be induced during very early stages of AD, prior to the formation of plaques and tangles [42, 43]. MAP-kinase is also involved in the regulation of γ-synuclein mRNA expression [44]. Analysis of the active phosphorylated form of mitogen activated protein kinase P44/42 MAPK (ERK1/2) showed that it is significantly induced in B103-695 cells while the non-phospho ERK levels were unaffected by APP expression (Fig 5b). Given potential crosstalk between PKA and MAPK signaling, we also investigated the impact of siRNA-mediated knockdown and chemical inhibition of PKA and found no effect on ERK phosphorylation status (data not shown). These findings suggest that APP expression specifically affects activation of ERK and do not have any effect on the expression of the protein.

Down-regulated proteins in this pathway (Fig 4) include PD2 and LIM domain 1 (PDLIM1) protein, a transcription regulator that has been shown to be responsive to hypoxia and also oxidative stress [45]. Differential PDLIM1 mRNA expression in human vastus lateralis muscle has been associated with Huntington's disease, making PDLIM1 a potential biomarker [46]. SYNCRIP is a member of the heterogeneous nuclear ribonucleoprotein (hnRNP) family, and was recently identified in a microarray study as a gene potentially involved in AD [47]. Our SILAC study provides additional evidence for these potential markers of AD at the protein level.

3.4 Implications in Alzheimer's Disease

Bioinformatic analysis of the 100 statistically significant proteins identified numerous proteins with roles in a variety of neurological diseases. We have listed differentially expressed proteins from our SILAC analysis that have been implicated in neurodegenerative disease in Table 1, reporting only those proteins with ratios having less than 30% relative standard deviation values. For example, hypoxanthine phosphoribosyltransferase 1 (HPRT1) was increased 10 fold and nerve growth factor receptor (NGFR) was increased 3.5 fold, and both of these proteins have been associated with neurodegeneration [48]. Nerve growth factor receptor as well as γ-synuclein also have emerging roles in AD [49]. There are two different types of nerve growth factor receptors; the low affinity nerve growth factor receptor, also known as $p75^{NTR}$, which binds all neurotrophins and the Trk family of tyrosine kinase receptors which bind specific neurotrophins. Both of these receptors have been associated with neurodegeneration and implicated in AD pathology as these receptors bind amyloid β, and are upregulated in AD [50, 51].

B103 cells expressing APP showed a decrease in Reticulon 4 (RTN4), an endoplasmic reticulum (ER) associated protein that is involved in neuroendocrine secretion. RTN4 has been shown to inhibit neurite outgrowth, and consequently has also been named neurite outgrowth inhibitor or Nogo. Increased expression of RTN4 has been shown to decrease amyloid-β peptide production by reducing β-amyloid converting enzyme 1 (BACE1) activity [52]. Park and colleagues found that RTN4 and its receptor RTN4R demonstrate

altered subcellular localization in AD. In normal brain RTN4 shows reduced cellular and enhanced neuropil localization whereas in AD brain it shows enhanced cellular localization. Similarly, while RTN4R is mainly localized to cell soma in normal brain it showed reduced cellular localization with more diffused staining in the neuropil and plaques in AD brain. RTN4R was also found to physically interact with APP and amyloid-β, limiting amyloid-β accumulation [53]. Another protein that showed downregulation in the B103-695 cells is the eukaryotic translation initiation factor 4A2 (eIF4A2), which showed a 7.98 fold decrease and is also associated with the ER. A decrease in expression of the proteins associated with ER may indicate that expression of APP leads to an induction of ER stress. ER responds to stress by activating various signaling pathways including the unfolded protein response (UPR), which leads to attenuation of protein translation. Studies have shown that APP induces ER stress-mediated apoptosis in cells and further studies are necessary to confirm that APP expression in B103 cells lead to an induction in ER stress-associated signaling pathways [54]. In AD, ER stress has been shown to induce inflammation, which leads to enhanced pathology development in AD. eIF4A2 has been suggested as one of 2 suitable reference genes for RT-qPCR studies in human AD post mortem brain samples, as its mRNA is stably expressed [55].

Analyses of AD brains have shown aberrant expression of cell cycle regulatory proteins in neurons. The roles of the cell cycle regulators in neurons as well as the mechanisms that lead to the induced expression of these proteins are not known. It is possible that either APP or a metabolite of APP may enhance expression of proteins such as γ-synuclein and Ras, thus affecting cell proliferation in transformed cells and degeneration in terminally differentiated cells. γ-synuclein has already been shown to bind and alter microtubule dynamics. Our co-immunostaining analysis with actin and γ-synuclein antibodies show altered localization of actin in the cells expressing APP. This is a significant finding and suggests that APP-mediated induction in γ-synuclein may lead to alterations in cytoskeletal and microtubule-associated proteins, which in turn affects neuronal signaling and synaptic function in AD. Since γ-synuclein affects the mitotic checkpoint, it is possible that the neuronal expression of this protein may not only alter the neuronal cytoskeleton but also affect the differentiation state of neurons. Neurons are terminally differentiated cells and do not have an active cell cycle machinery and therefore may respond to cell cycle activation by undergoing apoptosis instead of transformation. In addition to a role in AD, studies from different groups have shown that cancers of different organs show increased levels of APP or a metabolite of APP. Thus, a careful analysis of APP function may enhance our knowledge on the role of APP in bringing about pathologies associated with not only AD but also cancers of different organs.

4. Concluding Remarks

This study represents the first comprehensive proteomic analysis of B103 and B103-695 rat neuronal-like cells, including relative quantitation of protein expression using SILAC-based proteomics. Several proteins were identified as being significantly upregulated or downregulated in B103-695 cells, many with potential implications in AD pathology. The comprehensive dataset provides insight into proteins that may be affected by APP-695 expression and provides a foundation for future mechanistic studies. The proteins identified are associated with a number of diverse processes including cellular assembly and organization, cell cycle, lipid metabolism, protein folding, post translational modifications, as well as physiological system development and function. These findings suggest that several different processes are influenced by APP expression, which may contribute to synaptic dysfunction, amyloid plaque formation, and AD pathology.

Supplementary Material

Refer to Web version on PubMed Central for supplementary material.

Acknowledgments

This research was supported by grants from the Alzheimer's association (IIRG-08-90842 to JP), NIH-NIA (1R21AG031429-01A2 to JP) and funds from the USF Health Byrd Alzheimer's Institute, Department of Molecular Medicine, and Department of Cell Biology, Microbiology, and Molecular Biology at USF, Tampa. We thank Dr. Jeremiah Tipton and the Center of Drug Discovery and Innovation Proteomics Facility for use of the Orbitrap XL mass spectrometer. We also thank Dr. Bonnie Goodwin, who received the B103 cells from Dr. Dave Schubert at Salk Institute, for cells used in this study.

Abbreviations

SILAC	stable isotope labeling by amino acids in cell culture
APP	amyloid precursor protein
AD	Alzheimer’s disease
MS	Mass spectrometry

References

1. Kosik KS, Joachim CL, Selkoe DJ. Proc Natl Acad Sci U S A. 1986; 83:4044–4048. [PubMed: 2424016]
2. Selkoe DJ. Neuron. 1991; 6:487–498. [PubMed: 1673054]
3. Alzheimer A, Stelzmann RA, Schnitzlein HN, Murtagh FR. Clin Anat. 1995; 8:429–431. [PubMed: 8713166]
4. Naslund J, Schierhorn A, Hellman U, Lannfelt L, Roses AD, Tjernberg LO, Silberring J, Gandy SE, Winblad B, Greengard P, et al. Proc Natl Acad Sci U S A. 1994; 91:8378–8382. [PubMed: 8078890]
5. Iwatsubo T, Odaka A, Suzuki N, Mizusawa H, Nukina N, Ihara Y. Neuron. 1994; 13:45–53. [PubMed: 8043280]
6. Mori H, Takio K, Ogawara M, Selkoe DJ. J Biol Chem. 1992; 267:17082–17086. [PubMed: 1512246]
7. Duff K, Eckman C, Zehr C, Yu X, Prada CM, Perez-tur J, Hutton M, Buee L, Harigaya Y, Yager D, Morgan D, Gordon MN, Holcomb L, Refolo L, Zenk B, Hardy J, Younkin S. Nature. 1996; 383:710–713. [PubMed: 8878479]
8. Suzuki N, Cheung TT, Cai XD, Odaka A, Otvos L Jr, Eckman C, Golde TE, Younkin SG. Science. 1994; 264:1336–1340. [PubMed: 8191290]
9. Hernandez-Ortega K, Ferrera P, Arias C. J Neurosci Res. 2007; 85:1744–1751. [PubMed: 17455309]
10. Judge M, Hornbeck L, Potter H, Padmanabhan J. Mol Neurodegener. 2011; 6:80. [PubMed: 22112898]
11. Suzuki T, Oishi M, Marshak DR, Czernik AJ, Nairn AC, Greengard P. Embo J. 1994; 13:1114–1122. [PubMed: 8131745]
12. Lee MS, Kao SC, Lemere CA, Xia W, Tseng HC, Zhou Y, Neve R, Ahlijanian MK, Tsai LH. J Cell Biol. 2003; 163:83–95. [PubMed: 14557249]
13. Shin RW, Ogino K, Shimabuku A, Taki T, Nakashima H, Ishihara T, Kitamoto T. Acta Neuropathol. 2007; 113:627–636. [PubMed: 17431643]
14. Ueberham U, Hilbrich I, Ueberham E, Rohn S, Glockner P, Dietrich K, Bruckner MK, Arendt T. Neurobiol Aging. 2012
15. Bowser R, Smith MA. J Alzheimers Dis. 2002; 4:249–254. [PubMed: 12226545]
16. Busser J, Geldmacher DS, Herrup K. J Neurosci. 1998; 18:2801–2807. [PubMed: 9525997]

17. Andorfer C, Acker CM, Kress Y, Hof PR, Duff K, Davies P. J Neurosci. 2005; 25:5446–5454. [PubMed: 15930395]
18. Herrup K, Arendt T. J Alzheimers Dis. 2002; 4:243–247. [PubMed: 12226544]
19. Jordan-Sciutto K, Rhodes J, Bowser R. Mech Ageing Dev. 2001; 123:11–20. [PubMed: 11640947]
20. Malik B, Currais A, Andres A, Towlson C, Pitsi D, Nunes A, Niblock M, Cooper J, Hortobagyi T, Soriano S. Cell Cycle. 2008; 7:637–646. [PubMed: 18239458]
21. McShea A, Harris PL, Webster KR, Wahl AF, Smith MA. Am J Pathol. 1997; 150:1933–1939. [PubMed: 9176387]
22. Schubert D, Behl C. Brain Res. 1993; 629:275–282. [PubMed: 7906601]
23. Jin L, Ninomiya H, Roch J, Schubert D, Masliah E, Otero D, Saitoh T. The Journal of Neuroscience. 1994; 14:5461–5470. [PubMed: 8083748]
24. Wisniewski JR, Zougman A, Nagaraj N, Mann M. Nat Methods. 2009; 6:359–362. [PubMed: 19377485]
25. Cox J, Mann M. Nat Biotech. 2008; 26:1367–1372.
26. Benjamini Y, Hochberg Y. Journal of the Royal Statistical Society. Series B (Methodological). 1995; 57:289–300.
27. Hutter-Paier B, Huttunen HJ, Puglielli L, Eckman CB, Kim DY, Hofmeister A, Moir RD, Domnitz SB, Frosch MP, Windisch M, Kovacs DM. Neuron. 2004; 44:227–238. [PubMed: 15473963]
28. Temel RE, Gebre AK, Parks JS, Rudel LL. Journal of Biological Chemistry. 2003; 278:47594–47601. [PubMed: 12975367]
29. Nikolic M, Dudek H, Kwon YT, Ramos YF, Tsai LH. Genes Dev. 1996; 10:816–825. [PubMed: 8846918]
30. Tsai LH, Takahashi T, Caviness VS Jr, Harlow E. Development. 1993; 119:1029–1040. [PubMed: 8306873]
31. Su SC, Tsai LH. Annu Rev Cell Dev Biol. 2011; 27:465–491. [PubMed: 21740229]
32. Rakic S, Davis C, Molnar Z, Nikolic M, Parnavelas JG. Cereb Cortex. 2006; 16(Suppl 1):i35–i45. [PubMed: 16766706]
33. Rockenstein E, Hansen LA, Mallory M, Trojanowski JQ, Galasko D, Masliah E. Brain Res. 2001; 914:48–56. [PubMed: 11578596]
34. Zhang H, Kouadio A, Cartledge D, Godwin AK. Exp Cell Res. 2011; 317:1330–1339. [PubMed: 20974125]
35. Ji H, Liu YE, Jia T, Wang M, Liu J, Xiao G, Joseph BK, Rosen C, Shi YE. Cancer Res. 1997; 57:759–764. [PubMed: 9044857]
36. Jia T, Liu YE, Liu J, Shi YE. Cancer Res. 1999; 59:742–747. [PubMed: 9973226]
37. Inaba S, Li C, Shi YE, Song DQ, Jiang JD, Liu J. Breast Cancer Res Treat. 2005; 94:25–35. [PubMed: 16142440]
38. Gupta A, Inaba S, Wong OK, Fang G, Liu J. Oncogene. 2003; 22:7593–7599. [PubMed: 14576821]
39. Lüth HJ, Holzer M, Gertz HJ, Arendt T. Brain Res. 2000; 852:45–55. [PubMed: 10661494]
40. Tinhofer I, Maly K, Dietl P, Hochholdinger F, Mayr S, Obermeier A, Grunicke HH. Journal of Biological Chemistry. 1996; 271:30505–30509. [PubMed: 8940018]
41. Ferrer I, Blanco R, Carmona M, Ribera R, Goutan E, Puig B, Rey MJ, Cardozo A, Viñals F, Ribalta T. Brain Pathology. 2001; 11:144–158. [PubMed: 11303790]
42. Gärtner U, Holzer M, Heumann R, Arendt T. NeuroReport. 1995; 6:1441–1444. [PubMed: 7488744]
43. Gärtner U, Holzer M, Arendt T. Neuroscience. 1999; 91:1–5. [PubMed: 10336054]
44. Li M, Yin Y, Hua H, Sun X, Luo T, Wang J, Jiang Y. Journal of Biological Chemistry. 2010; 285:30480–30488. [PubMed: 20670935]
45. Basu A, Drame A, Muñoz R, Gijsbers R, Debyser Z, De Leon M, Casiano CA. The Prostate. 2012; 72:597–611. [PubMed: 21796653]

46. Strand AD, Aragaki AK, Shaw D, Bird T, Holton J, Turner C, Tapscott SJ, Tabrizi SJ, Schapira AH, Kooperberg C, Olson JM. Human Molecular Genetics. 2005; 14:1863–1876. [PubMed: 15888475]
47. Guttula SV AA, Gumpeny RS. International Journal of Alzheimer's Disease. 2012; 2012
48. Terrisse L, Poirier J, Bertrand P, Merched A, Visvikis S, Siest G, Milne R, Rassart E. J Neurochem. 1998; 71:1643–1650. [PubMed: 9751198]
49. Navarro A, del Valle E, Astudillo A, González del Rey C, Tolivia J. Experimental Neurology. 2003; 184:697–704. [PubMed: 14769361]
50. Yaar M, Zhai S, Fine RE, Eisenhauer PB, Arble BL, Stewart KB, Gilchrest BA. Journal of Biological Chemistry. 2002; 277:7720–7725. [PubMed: 11756426]
51. Podlesniy P, Kichev A, Pedraza C, Saurat J, Encinas M, Perez B, Ferrer I, Espinet C. Am J Pathol. 2006; 169:119–131. [PubMed: 16816366]
52. Dasgupta P, Sun J, Wang S, Fusaro G, Betts V, Padmanabhan J, Sebti SM, Chellappan SP. Molecular and cellular biology. 2004; 24:9527–9541. [PubMed: 15485920]
53. Park JH, Gimbel DA, GrandPre T, Lee J-K, Kim J-E, Li W, Lee DHS, Strittmatter SM. The Journal of Neuroscience. 2006; 26:1386–1395. [PubMed: 16452662]
54. Takahashi K, Niidome T, Akaike A, Kihara T, Sugimoto H. J Neurochem. 2009; 109:1324–1337. [PubMed: 19476545]
55. Penna I, Vella S, Gigoni A, Russo C, Cancedda R, Pagano A. International Journal of Molecular Sciences. 2011; 12:5461–5470. [PubMed: 22016602]

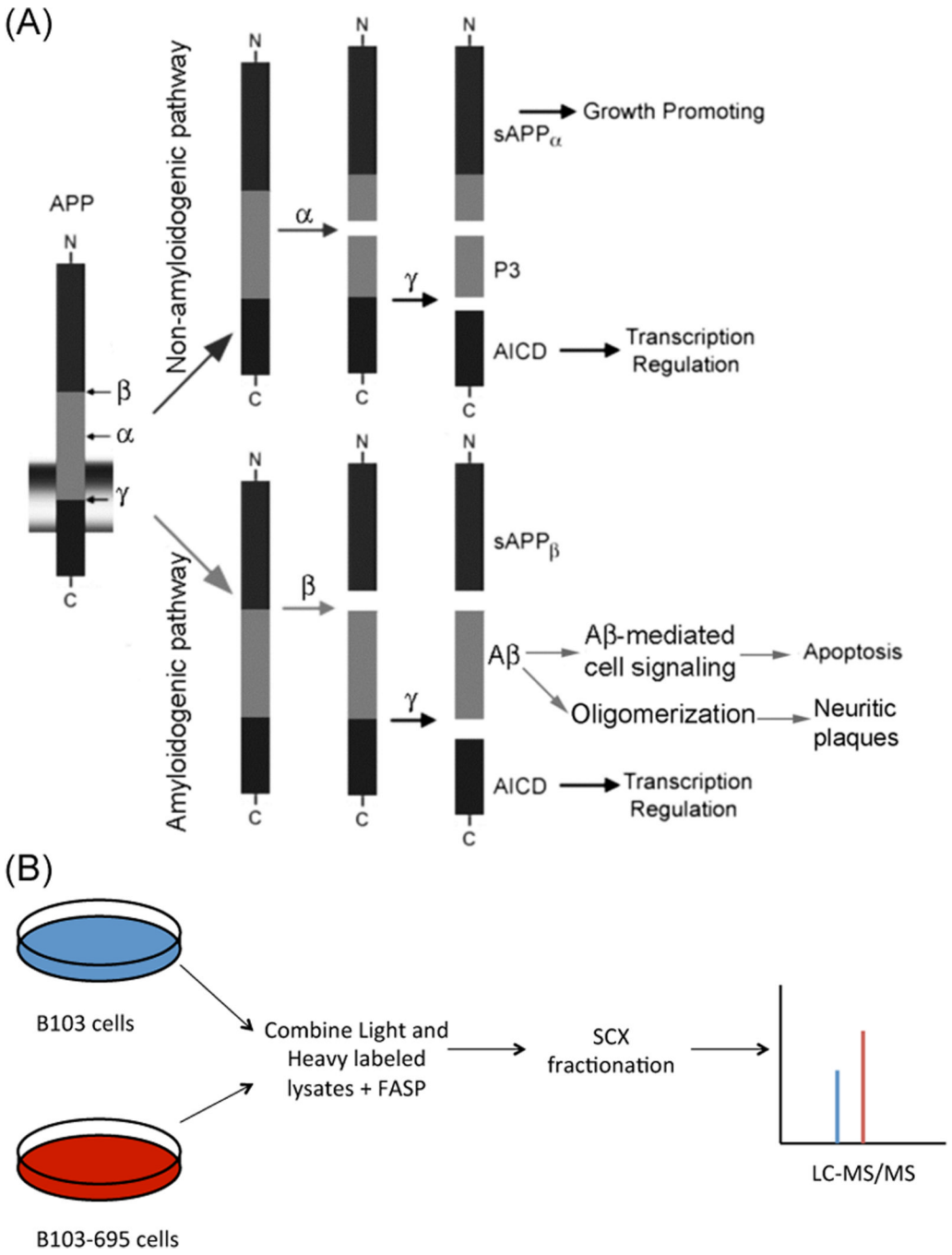

Figure 1.

a) Schematic of proteolytic processing of amyloid precursor protein (APP) by alpha, gamma, and beta secretases. b) SILAC experimental workflow used for differential protein expression profiling in B103 cells expressing APP-695.

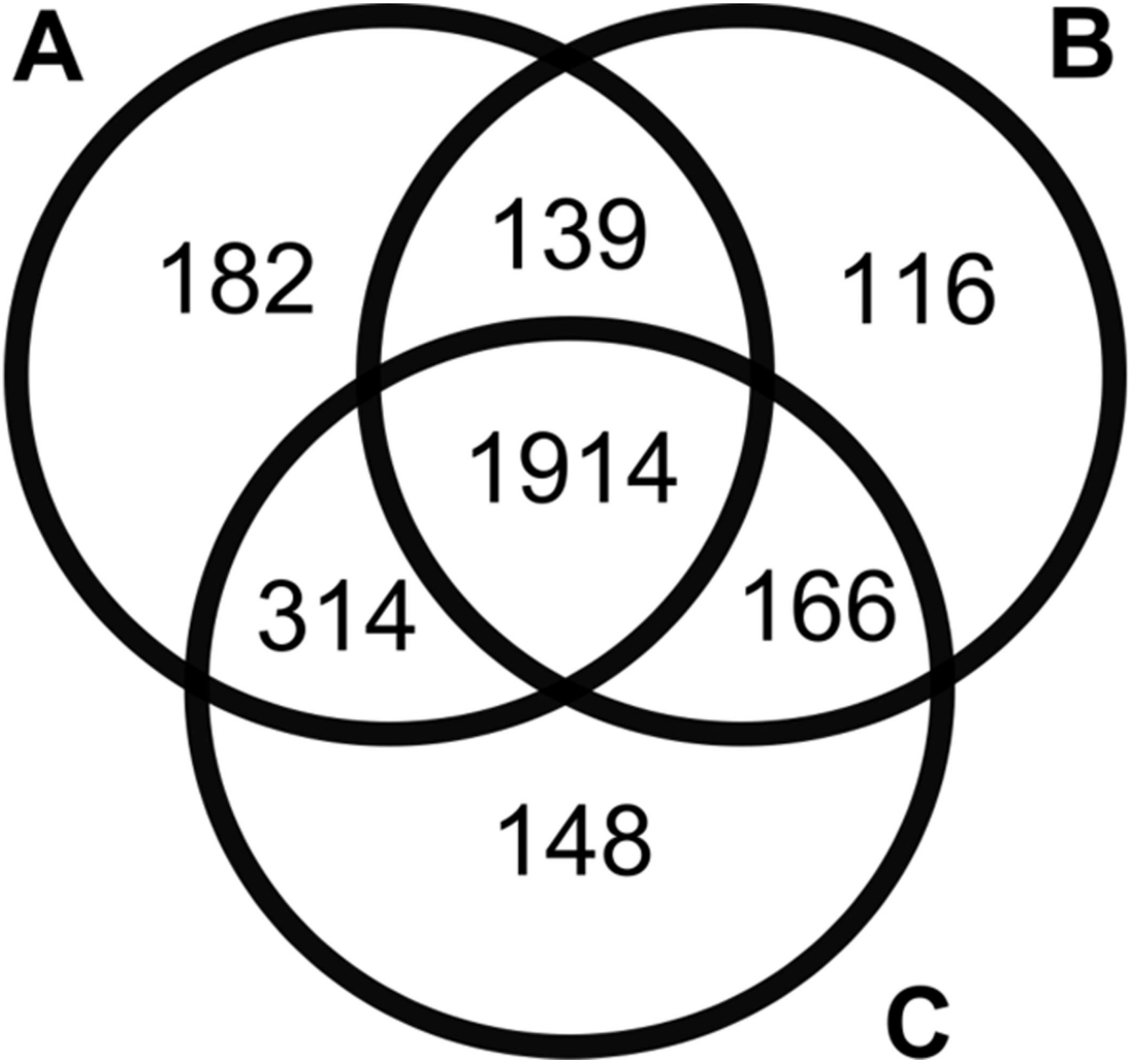

Figure 2.
Venn diagram representing the number of unique protein groups identified in biological replicate A, B, and C, and the overlap of proteins identified between the biological replicates.

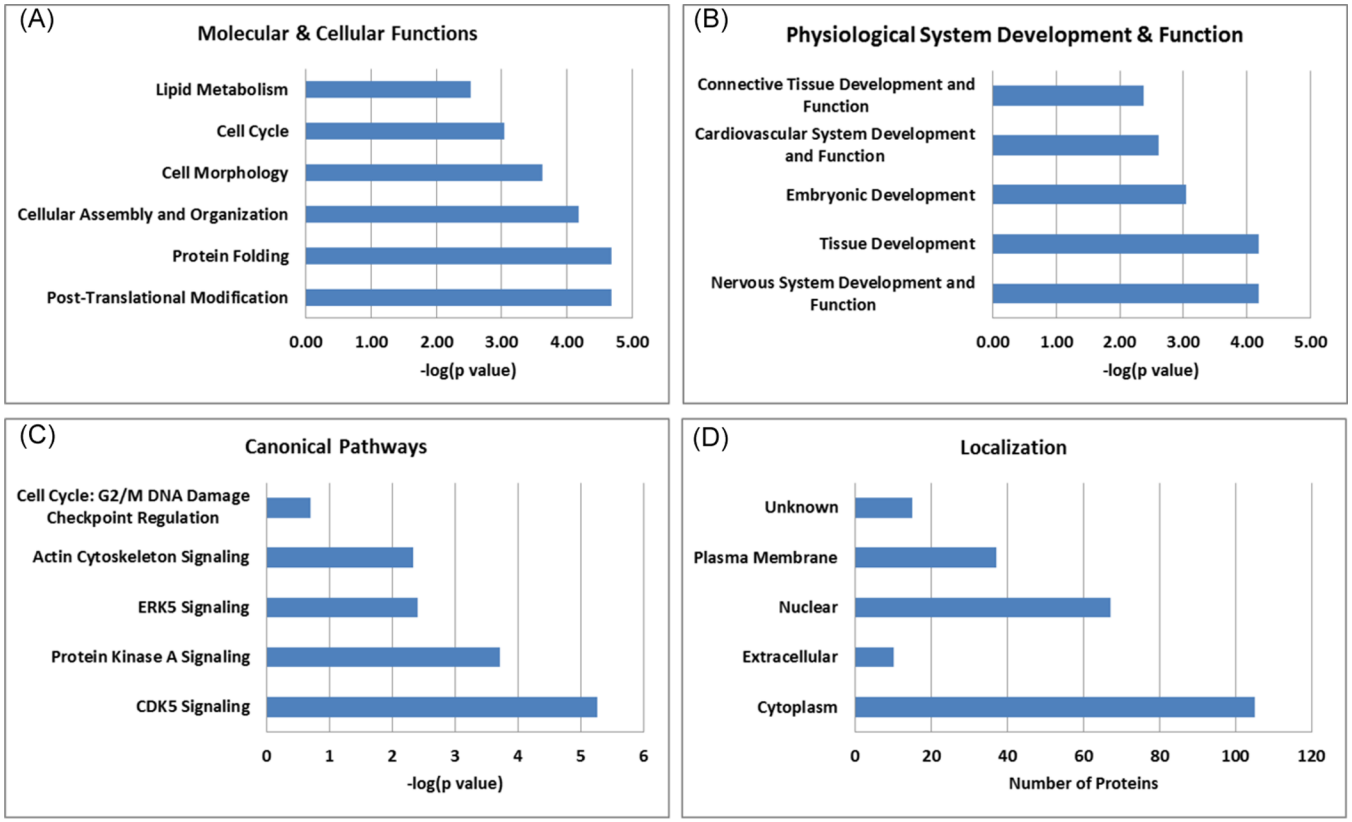

Figure 3.

Ingenuity Pathway Analysis of APP-mediated differential protein expression in B103 cells showing over-represented categories associated with a) molecular and cellular function, (b) physiological system development and function, (c) canonical pathways, and (d) cell localization.

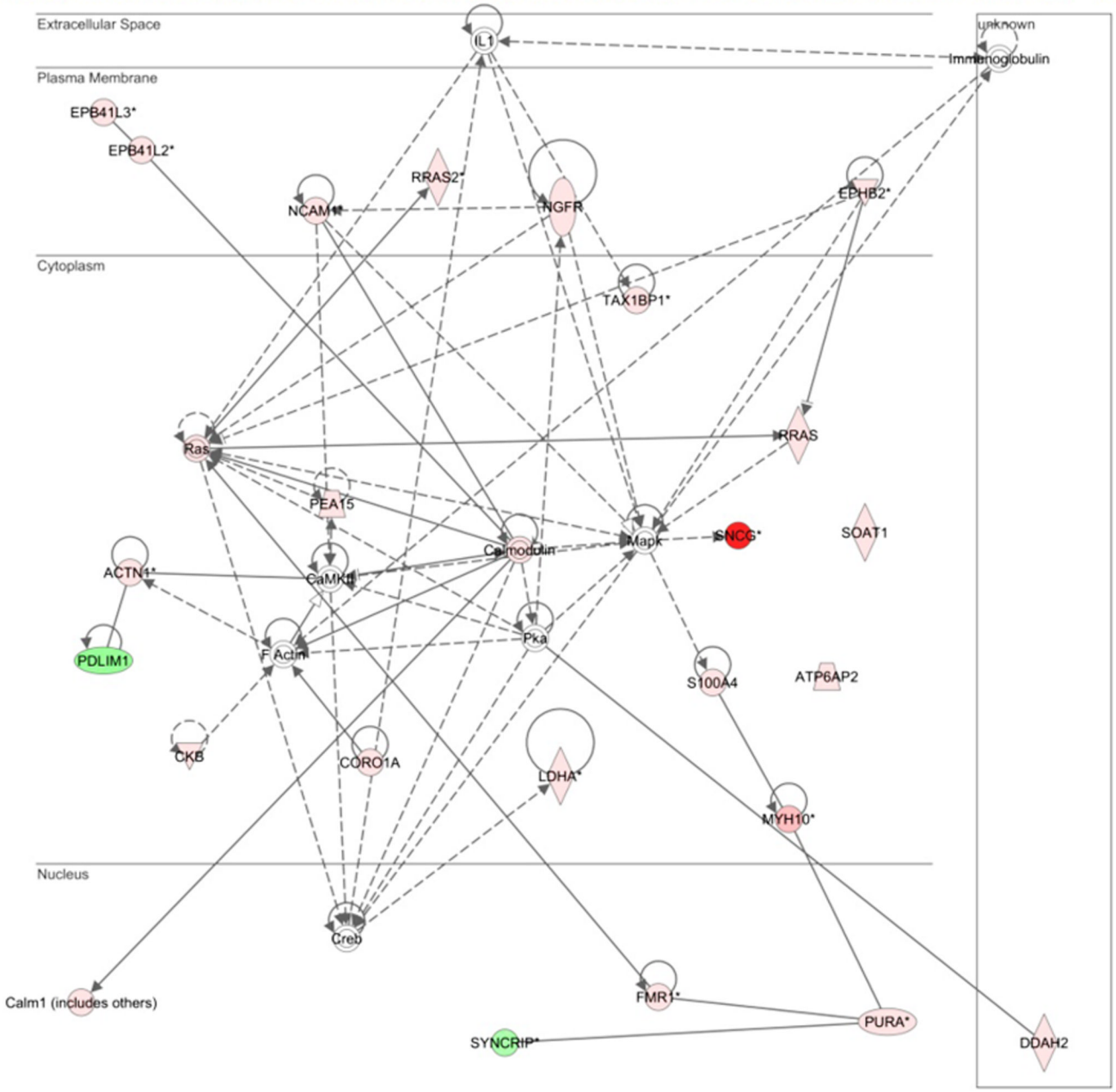

Figure 4.

Top-scoring pathway from Ingenuity Pathway Analysis associated with cellular assembly and organization based on differentially expressed proteins identified from B103 cells expressing APP-695. The network diagram uses different shapes to represent protein functions: enzymes (diamond), kinases (inverted triangle), transporters (trapezoid), and other (circles). Single lines represent protein-protein interactions; solid or dashed lines represent direct or indirect interactions, respectively. Proteins that regulate another protein are indicated by arrows.

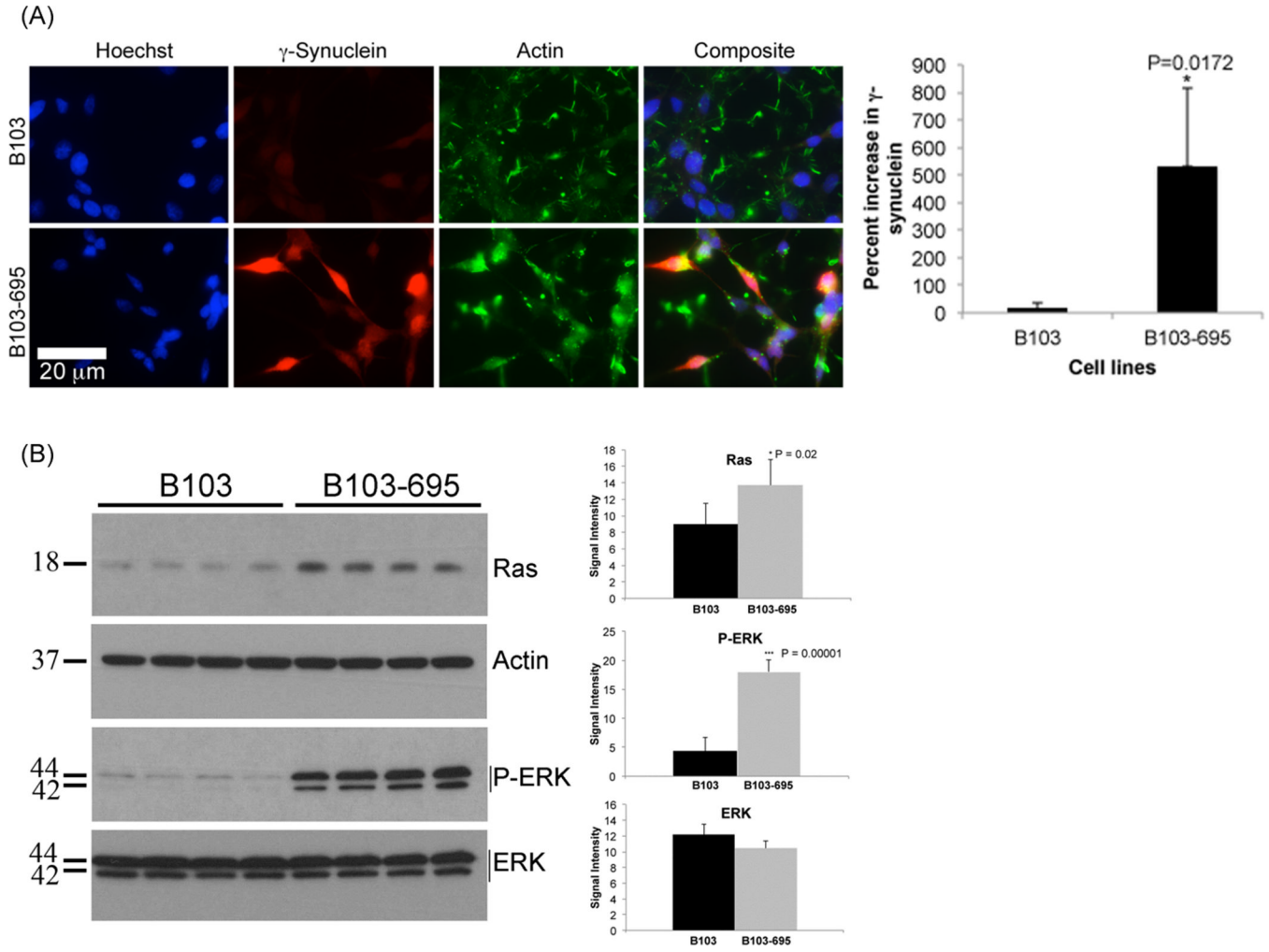

Figure 5.

(a) Immunostaining: B103 and B103-695 cells were co-immunostained using γ-synuclein (rabbit polyclonal) and actin (mouse monoclonal) primary antibodies and Alexa Fluor 594 anti-rabbit and Alexa Fluor 488 anti-mouse secondary antibodies. Hoechst was used to visualize the nuclei. The expression of γ-synuclein was significantly higher in B103-695 than that in B103 cells and it seems to localize to the nucleus and cytoplasm. Images were taken on a Zeiss fluorescent microscope fitted with an Axiocam MRm camera and analyzed using AxioVision Rel 4.8 software (magnification: 63×). The bar graph shows the percent increase in γ-synuclein intensity measured using ImageJ, image analysis tool, after converting the images to 8 bit gray. The intensity of γ-synuclein in three independent images taken from B103 and B103-695 cells were normalized to the intensity of Hoechst within the same sample for comparison. (b) Western blot validation: Equal amounts of proteins from B103 and B103-695 cell extracts done in quadruplicate were separated on a 15 % Tris-glycine gel and probed with Ras, and P-ERK antibodies. Both Ras and P-ERK were significantly increased in B103-695 cells compared to B103 cells (bar graphs labeled Ras and P-ERK). Re-probe of the Ras blot with actin antibody shows equal amount of proteins on gel and re-probe of P-ERK blot with ERK antibody shows no change in expression of ERK upon expression of APP (bar graph labeled ERK).

Table 1

Selected differentially expressed proteins implicated in neurodegenerative disease that were identified in B103–695 cells using SILAC-based quantitative proteomic analysis.

Fold Change	Standard Deviation	ID	Symbol	Entrez Gene Name	Location
59.650	10.17	F1LQ96	SNCG	synuclein, gamma (breast cancer-specific protein 1)	Cytoplasm
11.433	2.78	Q811A3	PLOD2	procollagen-lysine, 2-oxoglutarate 5-dioxygenase 2	Cytoplasm
8.363	0.78	F1LSL3	ITPR3	inositol 1,4,5-trisphosphate receptor, type 3	Cytoplasm
7.953	0.78	B2B9B0	EPHB2	EPH receptor B2	Plasma Membrane
4.284	0.65	D3ZZ63	FLNC	filamin C, gamma	Cytoplasm
3.819	0.41	F1MA96	NCAM1	neural cell adhesion molecule 1	Plasma Membrane
3.770	0.85	P50442	GATM	glycine amidinotransferase (L-arginine:glycine amidinotransferase)	Cytoplasm
3.638	0.52	F1LNX0	DDAH1	dimethylarginine dimethylaminohydrolase 1	Cytoplasm
3.547	0.21	Q5HZV9	PPP1R7	protein phosphatase 1, regulatory subunit 7	Nucleus
3.519	0.15	P07174	NGFR	nerve growth factor receptor	Plasma Membrane
2.970	0.59	P70636	LAMA5	laminin, alpha 5	Extracellular Space
2.872	0.27	Q6MG60	DDAH2	dimethylarginine dimethylaminohydrolase 2	unknown
2.768	0.17	F1M5W8	AFAP1L2	actin filament associated protein 1-like 2	Cytoplasm
2.765	0.08	P05942	S100A4	S100 calcium binding protein A4	Cytoplasm
2.657	0.43	F1LNU6	FADS2	fatty acid desaturase 2	Plasma Membrane
2.653	0.42	Q80WE1	FMR1	fragile X mental retardation 1	Nucleus
2.557	0.17	F1LYK7	CFL2	cofilin 2 (muscle)	Nucleus
2.375	0.40	F1LZM7	HSDL2	hydroxysteroid dehydrogenase like 2	Cytoplasm
2.317	0.19	D4A4T0	STUB1	STIP1 homology and U-box containing protein 1, E3 ubiquitin protein ligase	Cytoplasm
2.309	0.10	Q91ZN1	CORO1A	coronin, actin binding protein, 1A	Cytoplasm
2.298	0.22	F1LV02	DBI	diazepam binding inhibitor (GABA receptor modulator, acyl-CoA binding protein)	Cytoplasm
2.292	0.18	F1LND7	FDPS	farnesyl diphosphate synthase	Cytoplasm
2.206	0.17	Q68G41	ECI1	enoyl-CoA delta isomerase 1	Cytoplasm
2.156	0.38	Q4G053	SAMD9L	sterile alpha motif domain containing 9-like	unknown
2.144	0.16	P40615	DKC1	dyskeratosis congenita 1, dyskerin	Nucleus

Fold Change	Standard Deviation	ID	Symbol	Entrez Gene Name	Location
2.118	0.08	P10868	GAMT	guanidinoacetate N-methyltransferase	Cytoplasm
2.072	0.06	Q63081	PDIA6	protein disulfide isomerase family A, member 6	Cytoplasm
1.880	0.03	P13233	CNP	2',3'-cyclic nucleotide 3' phosphodiesterase	Cytoplasm
1.865	0.03	D4ABV5	Calm1	calmodulin 1	Nucleus
1.853	0.05	D3ZM53	Ywhaq	tyrosine 3-monooxygenase/tryptophan 5-monooxygenase activation protein, theta polypeptide	Cytoplasm
1.850	0.21	D4A2V9	GPI	glucose−6-phosphate isomerase	Extracellular Space
1.831	0.28	P16617	PGK1	phosphoglycerate kinase 1	Cytoplasm
1.819	0.13	P21263	NES	nestin	Cytoplasm
1.733	0.13	P07335	CKB	creatine kinase, brain	Cytoplasm
1.714	0.10	O35244	PRDX6	peroxiredoxin 6	Cytoplasm
−2.015	0.41	Q6URK4	HNRNPA3	heterogeneous nuclear ribonucleoprotein A3	Nucleus
−2.143	0.05	D4A8D5	FLNB	filamin B, beta	Cytoplasm
−2.342	0.03	F1M3G6	HSPH1	heat shock 105kDa/110kDa protein 1	Cytoplasm
−2.941	0.06	Q5U1Z3	RTN4	reticulon 4	Cytoplasm
−3.017	0.10	Q7TP47	SYNCRIP	synaptotagmin binding, cytoplasmic RNA interacting protein	Nucleus
−3.615	0.06	P52944	PDLIM1	PDZ and LIM domain 1	Cytoplasm
−7.977	0.07	F1LP27	EIF4A2	eukaryotic translation initiation factor 4A2	Cytoplasm

Electrophoresis. Author manuscript; available in PMC 2013 December 01.